ERJ Express. Published on September 3, 2008 as doi: 10.1183/09031936.00159507

Increased hyaluronic acid content in idiopathic pulmonary arterial hypertension

E. Papakonstantinou[1*], F.M. Kouri[2*], G. Karakiulakis[1], I. Klangas[1], O. Eickelberg[2†]

[1]Department of Pharmacology, Aristotle University School of Medicine, Thessaloniki, Greece; [2]Department of Medicine, University of Giessen Lung Center, Justus Liebig University, Giessen, Germany

[*]**The first two authors have contributed equally to this study**

[†]**To whom correspondence should be addressed:**

Oliver Eickelberg, MD

University of Giessen Lung Center

Department of Medicine II phone: +49 (641) 9942300

Aulweg 123, Room 6-11 fax: +49 (641) 9942309

D-35392 Giessen email: oliver.eickelberg@innere.med.uni-giessen.de

Eleni Papakonstantinou was recipient of a European Respiratory Society short-term fellowship (#382)

This work was supported by the German Research Foundation (DFG) Collaborative Research Center 547 (O.E.), the DFG-sponsored international graduate college SMLPD (F.M.K., O.E.), the Excellence cluster "Cardiopulmonary System" (ECCPS), and the General Secretariat for Research and Technology of Greece (# 03EΔ950).

Short title: HA expression in PAH

Abstract

Idiopathic pulmonary arterial hypertension (IPAH) is a fatal disease characterized by elevated blood pressure in the pulmonary circulation. Initial vasoconstriction, proliferation of pulmonary arterial smooth muscle cells (PASMC), and increased deposition of extracellular matrix (ECM) contribute to pathologic remodelling of pulmonary arterioles in IPAH. Glycosaminoglycans (GAG), components of the ECM, control cellular proliferation and differentiation, but their expression in IPAH remains elusive.

Here, we investigated GAG expression in lungs of patients with IPAH or control transplant donors, and analyzed expression and localization of GAG metabolizing enzymes *in vivo* and *in vitr*o. We detected a significant increase in the expression of hyaluronic acid (HA) in IPAH lungs, associated with increased hyaluronan synthase (HAS) 1 and decreased hyaluronoglucosaminidase (HYAL) 1 gene expression, assessed by quantitative (q)RT-PCR and Western blotting. HAS1 protein localized to PASMC *in vivo*, and increased HA deposition was observed in remodelled pulmonary arteries in IPAH. TGF-β1, a profibrotic growth factor, led to increased HA secretion and HAS1 expression in primary PASMC.

Our results demonstrate an increased HA content in IPAH lungs, associated with increased HAS1 and decreased HYAL1 gene expression. Synergistic regulation of GAG metabolizing enzymes in favour of accumulation may thus regulate pathologic vascular remodelling in IPAH lungs.

Keywords: hyaluronic acid, pulmonary arterial hypertension, TGF-β1, pulmonary arterial smooth muscle cells, vascular remodelling

Introduction

Idiopathic pulmonary arterial hypertension (IPAH) is a rare but fatal disease characterized by elevated blood pressure in the pulmonary circulation, due to increased vascular resistance of pulmonary arterioles [1, 2]. If untreated, IPAH leads to right ventricular hypertrophy, failure, and subsequent death. Early in disease pathogenesis, endothelial cell dysfunction triggers increased vasoconstriction and *in situ* thrombosis. This is followed by pathologic vascular remodelling, a process characterized by intimal fibrosis and thickening of the medial and adventitial layers, due to uncontrolled proliferation of pulmonary arterial smooth muscle cells (PASMC) and perivascular fibroblasts [3-5]. In parallel, enhanced cellular activation of PASMC and fibroblasts leads to excessive extracellular matrix (ECM) deposition, which potentiates the increased stiffness of pulmonary arteries in IPAH [6, 7].

Altered ECM turnover is a hallmark of several pulmonary diseases, including the adult respiratory distress syndrome, asthma, idiopathic pulmonary fibrosis, or chronic obstructive lung disease, which underlines the importance of ECM homeostasis for proper lung function [7-9]. In the lung, the ECM is subjected to a daily turnover of about 10% of total ECM, indicating that subtle changes in turnover rates accumulate to large changes in total ECM composition with time [10]. The ECM is largely composed of collagens, fibronectin, vitronectin, proteoglycans, and glycosaminoglycans (GAG) [11]. GAG are linear acidic polysaccharides of variable length and composition that are grouped into four major categories: hyaluronic acid (HA), heparin and heparan sulphate (HS), chondroitin and dermatan sulphates (CS, DS), and keratan sulphate (KS) [12, 13]. GAG have been previously shown to control lung inflammation, as well as the phenotype of systemic vascular smooth muscle cells [14-16].

HA is a major component of the basement membrane, and constitutes about 10% of all proteoglycans [17]. HA is synthesized at the inner surface of the plasma membrane by one or

more hyaluronan synthase isoforms (HAS1, HAS2, or HAS3), which exhibit distinct enzymatic properties and synthesize HA chains of various average chain length [18]. After synthesis, HA chains are extruded to pore-like structures into the extracellular space. On the other hand, HA can be degraded by one of four hyaluronoglucosaminidase isoforms (HYAL1 to HYAL4). HYAL1, the main hyaluronoglucosaminidase, exhibits the highest hyaluronidase activity and thus represents the major enzyme for HA degradation [19].

HA can influence cellular responses in several ways: First, the interaction of HA with pericellular macromolecules leads to softening of the ECM, thereby facilitating cell shape changes that are required for cell division, migration, or plasticity [20-22]. As a result, increased levels of HA have been implicated in inflammation, morphogenesis, regeneration, wound healing, tumor invasion, or cancer metastasis [21-23]. Second, HA can directly interact with the cell surface receptors CD44 and the receptor for hyaluronan-mediated motility (RHAMM), which directly transduce intracellular signalling cascades via extracellular signal-regulated kinase (ERK1/2) [12, 24, 25].

CD44 and HA expression was increased after lung injury induced by the DNA-damaging chemotherapeutic agent bleomycin, and mediated pro-inflammatory mediator release by alveolar macrophages [26]. Increased HA content was detected in atherosclerotic regions [20, 27, 28], and HA has been described to induce smooth muscle cell migration [29], altogether suggesting its potential involvement in remodeling of the systemic vasculature, but its contribution to pulmonary vascular remodeling in IPAH remains elusive. In this study, we investigated GAG expression in lung tissues of IPAH patients and control transplant donors, and analyzed the expression and localization of HA metabolizing enzymes in human lung samples and PASMC *in vivo* and *in vitr*o, respectively.

Materials and methods

Lung tissues and primary pulmonary arterial smooth muscle cells (PASMC)

Lung tissue samples were obtained during lung transplantation from twelve patients with IPAH (mean age 32 ± 10 years; 7 females, 5 males) and nine control subjects (organ donors, mean age 38 ± 14. years; 5 females, 4 males). None of the IPAH patients exhibited *BMPR2* mutations (table 1). For tissue processing, all samples were immediately placed in 4% (w/v) paraformaldehyde or liquid nitrogen after explantation. The study protocol was approved by the Ethics Committee of the Justus-Liebig-University School of Medicine (AZ 31/93). Informed consent was obtained from each subject for the study protocol. Primary PASMC were generated from arteries of IPAH or donor lungs derived from explanted lung tissues, as indicated, and prepared for isolation of PASMC, as previously described [30]. Cells were cultured in smooth muscle cell growth medium 2 (PromoCell, Heidelberg, Germany) at 37°C in 5% CO_2, 95 % O_2 atmosphere. Passages three to seven were used for the experiments.

GAG isolation and purification

Lung tissue specimens were homogenised at 4ºC using a Polytron homogenizer in 25 mM Tris–HCl, pH 7.6 (10 ml/g of tissue). Homogenized tissues were delipidated in chloroform/methanol (1:2 v/v). Organic solvents were removed by centrifugation (3.200 × g, 20 min, 4ºC) and the pellet was washed with 10 ml of ethanol, centrifuged as described above, and dried at 40ºC for 4 h. The remaining pellet was then resuspended in 0.1 M Tris-HCl, pH 8.0, 1 mM $CaCl_2$ and GAG were isolated and purified following digestion with pronase (*Streptomyces griseus*, EMD Chemicals Inc., San Diego, CA, USA), DNase I (EC 3.1.21.1, Calbiochem) and β-elimination in the presence of 1 M $NaBH_4$ [20]. Total GAG were

precipitated with four volumes of ethanol in the presence of 0.1 volume of 3 M CH_3COONa overnight at -4ºC, recovered with centrifugation (20 min, 2.000 × g), dissolved in double distilled H_2O, and stored at 4ºC. Colorimetric determination of uronic acids was performed as reported [31].

Cellulose acetate electrophoresis

Two µl GAG solution, containing 4 µg of uronic acids, were subjected to cellulose acetate electrophoresis in 100 mM pyridine / 470 mM formic acid, pH 3.0, using 7 mA constant current, at room temperature, for 70 min. Commercially available GAG standards used as markers included: HA, heparan sulphate (HS), dermatan sulphate (DS), and chondroitin sulphate CS) (all from Sigma-Aldrich, St. Louis, MO, USA). After electrophoresis, the cellulose acetate strip was stained with 0.2% Alcian blue (w/v), in 0.1% acetic acid (v/v), for 10 min and washed with 0.1% acetic acid (v/v) for 20 min [20]. Staining intensity was quantified using a computer-assisted image analysis programme according to the manufacturer's recommendation (Eastman Kodak, Rochester, NY, USA).

GAG characterization

Speed-dried GAG (5 µg of uronic acids) were incubated in a final volume of 15 µl with the following enzymes: (a) Heparinase: samples were dissolved in 100 mM Tris-HCl buffer, pH 7.0, containing 3 mM $CaCl_2$ and incubated with 4×10^{-4} U of heparin lyase I (EC 4.2.2.7, *Flavobacterium heparinum*, Seikagaku, Tokyo, Japan), for 15 h at 30ºC. (b) Heparitinase: samples were dissolved as above and incubated with 4×10^{-4} U of heparan sulphate lyase (heparitinase: EC 4.2.2.8, *Flavobacterium heparinum*, Seikagaku) for 16 h at 43ºC. (c) Chondroitinase ABC: samples were dissolved in 100 mM Tris-HCl buffer, pH 8.0, containing 50 mM sodium acetate were incubated with 2×10^{-4} U of chondroitin ABC lyase (EC 4.2.2.4,

Proteus vulgaris, Sigma) for 16 h, at 37ºC. (d) Chondroitinase B: samples dissolved in 100 mM Tris-HCl buffer, pH 7.4, were incubated with 0.1 U of chondroitin B lyase (*Flavobacterium heparinum*, Seikagaku) for 16 h at 37ºC. (e) Keratanase: samples were dissolved in 50 mM Tris-HCl buffer, pH 7.4 and incubated with 0.05 U of keratan sulphate endo-β-D-galactosidase (EC 3.2.10.3, Pseudomonas species, Sigma-Aldrich) for 16 h at 37^{o}C. (f) Hyaluronidase: samples were dissolved in 20 mM sodium acetate, buffered with acetic acid to pH 5.0, and incubated with 4 U of hyaluronate lyase (EC 4.2.2.1, *Streptomyces hyalurolyticus*, Seikagaku) for 14 h at 60ºC. Incubation times and enzyme concentrations were as required for complete degradation of standard substrates, as published [32].

HA measurements

To analyze secreted hyaluronic acid, primary PASMC were grown to subconfluence in 24-well plates. Cells were then stimulated with TGF-β1 (0.2, 2, or 10 ng/ml, as indicated) for 6, 12, or 24 h. At the end of incubation time, aliquots of culture media were removed and HA content measured by EIA according to the manufacturer's instructions (Corgenix, Westminster, CO). Similarly, HA content in lung specimen and cell lysates were determined by EIA. To measure *de novo* GAG synthesis, subconfluent primary PASMC were incubated for 24 h in the presence or absence of TGF-β1 (0.2 or 2 ng/ml, as indicated), BMP-2 (10 or 20 ng/ml, as indicated), the type I TGF-β receptor kinase inhibitor SB431542 (10 μM), the p38 inhibitor SB203580 (10 μM), or PDGF-BB (10 ng/ml). The [^{3}H]-glucosamine (0.5 μCi/ml) (Amersham Corp., Buckinghamshire, UK) was then added to culture media for another 24 h. Culture media and cell layers were then collected and digested with 0.1 KU of Pronase (*Streptomyces griseus,* EMD Chemicals Inc.). Total GAG were precipitated by adding a mixture of ethanol (80% final concentration), containing 1.3% (w/v) sodium acetate. The samples were stored at -20^{o}C overnight and centrifuged at 10.000 × g, pellets dissolved in 0.5

M NaOH, and total GAG synthesis measured by liquid scintillation counting, as previously described [16].

Immunohistochemistry

Human paraffin-embedded lung specimen (3 μm) from healthy donors or IPAH patients were stained with biotinylated hyaluronan binding protein (HABP; Seigakaku), α-SMA (Sigma-Aldrich), α-HYAL1 (Novus Biologicals, Littleton, CO), or α-HAS1 (both from Santa Cruz Biotechnology, Santa Cruz, CA, USA) antibodies using the Histostain *Plus* Kit (Zymed, San Francisco, USA), as previously described [30]. Sections pre-incubated with 50 U/ml of hyaluronate lyase (EC 4.2.2.1, *Streptomyces hyalurolyticus*, Seikagaku) for 3 h at 37^{o}C, or sections incubated with isotype-matched pre-immune serum, served as negative controls for HABP and SMA, HYAL-1, or HAS1 immunostaining, respectively.

Quantitative reverse transcriptase (RT)-PCR

Total RNA was extracted using Qiagen extraction kits according to the manufacturer's protocol, and cDNAs were generated by reverse transcription using SuperScript™ II (Invitrogen, Carlsbad, CA, USA). Quantitative PCR was performed using fluorogenic SYBR Green and the Sequence Detection System 7700 (PE Applied Biosystems, Foster City, CA, USA) [30]. Human *hydroxymethylbilane synthase* (*Hmbs*), a ubiquitously and equally expressed gene free of pseudogenes, was used as reference gene in all qRT-PCR reactions. PCRs were performed using the primers listed in table 2 at a final concentration of 200 nM. Relative transcript abundance of a gene is expressed in ΔCt values ($\Delta Ct = Ct_{reference} - Ct_{target}$), as previously described in detail [30].

Results

Expression of GAG in IPAH

Electrophoretic analysis of total GAG isolated and purified from lung tissue specimens from IPAH patients or healthy donors revealed the presence of four distinct GAG populations (G1, G2, G3, and G4) in donor and IPAH lungs (fig. 1a). Enzymatic treatment with specific GAG-degrading enzymes (table 3), as well as comparison with the electrophoretic mobility of commercially available GAG standards (fig. 1a), identified G1 as hyaluronic acid (HA), G2 as heparan sulphate (HS), G3 as dermatan sulphate (DS), and G4 as chondroitin sulphate (CS). Densitometric analysis of alcian blue staining of these GAG revealed a significant increase in HA content, and a significant decrease in the content of HS, DS, or CS in IPAH tissue specimens, as compared with donors (fig. 1b). In order to further quantify the increase in HA, we measured the HA concentration within total GAG in lung specimens by EIA. As shown in fig. 1c, the relative amount of HA in the lungs of IPAH patients was significantly increased, compared with lung tissues from transplant donors (78.6 ± 7.83 versus 43.175 ± 6.87 ng/μg of total uronic acids for IPAH and donor lungs, respectively).

Localization of GAG in IPAH

To further localize HA, and its main metabolizing enzymes hyaluronan synthase (HAS) 1 and hyaluronoglucosaminidase (HYAL) 1 in the lungs of IPAH patients or transplant donors, immunohistochemical stainings were performed next. As depicted in fig. 2, HA expression could be detected throughout the alveolar interstitium, in the perivascular and peribronchiolar adventitia, and the endothelium. In remodeled lesions in IPAH, HA also frequently localized to subendothelial areas that stained negative for smooth muscle actin

(arrowheads, fig. 2, lower panels), indicating that it is expressed in areas of dedifferentiated PASMC. In contrast, HAS1 and HYAL1 expression was dominant in PASMC, suggesting that HA is synthesized by PASMC, and subsequently secreted towards the adventitia. While HYAL1 expression was attenuated in IPAH, significant HYAL1 expression was retained in bronchial and alveolar epithelial type II cells (arrows, fig. 2, upper panels). Stainings using tissue sections pre-digested with hyaluronidase, or using species-matched isotype controls, exhibited no staining, indicating specificity of the antibodies used (data not shown).

Expression of GAG metabolizing enzymes in IPAH in vivo and PASMC in vitro

Since both the expression and average size of HA was increased in IPAH, we next quantified *Has* and *Hyal* mRNA expression in lung tissue specimens and primary PASMC using qRT-PCR. As depicted in fig. 3a, *Has1-3*, *Hyal1-3*, *CD44*, and *Rhamm* were all expressed in the human lung, while *Hyal4* mRNA was expressed only at very low levels. When comparing expression levels in donor and IPAH lungs, we detected significantly increased expression levels of *Has1* and *CD44*, but decreased levels of *Hyal1* in IPAH (fig. 3a). We confirmed increased HAS1 protein expression in IPAH lungs by Western blot analysis (fig. 3b).

As our immunohistochemical data (fig. 2) indicated that HAS1 and HYAL1 were localized to PASMC *in vivo*, and PASMC represent a key pathogenic cell type in IPAH, we next isolated primary PASMC from IPAH and donor patients, and assessed *Has1* and *Hyal1* mRNA expression by qRT-PCR (fig. 4). While we did not observe any differences in *Has1* mRNA expression, *Hyal1* expression levels were significantly attenuated in primary PASMC obtained from IPAH patients compared with donors, thus reflecting the changes we observed upon analysis of lung homogenates (compare fig. 3a and 4).

Secretion and deposition of GAG by PASMC

Since *i*) IPAH is characterized by increased ECM deposition by PASMC, *ii*) TGF-β1 is a key regulator of ECM deposition, and *iii*) increased HA staining was observed in vessels of IPAH patients (fig. 2), we next investigated the effect of TGF-β1 on total GAG secretion and deposition in primary PASMC using [^{3}H]-glucosamine incorporation studies. As shown in figure 5a, both PDGF-BB and TGF-β1 significantly enhanced secretion of total GAG by PASMC. TGF-β1 at 2 ng/ml also significantly induced deposition of GAG into the provisional ECM deposited by PASMC. In contrast, BMP-2 did not affect GAG synthesis by PASMC (fig. 5a).

In order to further elucidate TGF-β1-induced signal transduction pathways controlling GAG synthesis, PASMC were pre-incubated with specific inhibitors of the TGF-β type I receptor (SB431542) or p38 MAPK (SB203580), and TGF-β1-dependent [^{3}H]-glucosamine incorporation was assessed (fig. 5b). Pre-treatment with either SB431542 or SB203580 led to a significant inhibition of basal and TGF-β1-induced GAG secretion. In addition, SB431542 or SB203580 pre-treatment inhibited TGF-β1-induced, but not basal, GAG deposition by PASMC (fig. 5b).

Secretion of HA by PASMC

In order to further investigate whether the TGF-β1-dependent increase of [^{3}H]-glucosamine incorporation is in part a result of increased HA secretion, we next measured HA secretion by PASMC by EIA. As depicted in figure 6, PASMC secreted considerable amounts of HA under baseline conditions, which was significantly enhanced by TGF-β1 in a time-dependant manner. While high TGF-β1 concentrations (10 ng/ml) led to a significant increase of HA secretion already after 12 hours, physiological concentrations of TGF-β1 (0.2 - 2 ng/ml) significantly increased HA secretion by PASMC after 24 h (fig. 6).

Expression of GAG metabolizing enzymes in PASMC

The time course of TGF-β1-induced HA secretion indicated that *de novo* gene expression of *Has1-3*, or repression of *Hyal1-3*, may be required for this increase. We therefore next assessed *Has* and *Hyal* mRNA expression in primary human PASMC that were stimulated with TGF-β1 for up to 6 hours. Using qRT-PCR, we detected a significant increase of *Has1* gene expression as early as 2 h after TGF-β1 stimulation of PASMC, which was even further increased after 6 h (fig. 7). In contrast, TGF-β1 had no significant effect on the expression of *Has2-3*, *Hyal1-3*, *CD44*, or *Rhamm* (fig. 6). Of interest, *Hyal4* was not expressed in PASMC and is therefore not included in fig. 7.

Discussion

Despite major recent advances in the pathophysiology, diagnosis, and therapy of idiopathic pulmonary hypertension (IPAH), the molecular mechanisms underlying endothelial and smooth muscle cell dysfunction in this disease remain to be fully elucidated [4]. Initial endothelial dysfunction contributes to impaired vasoregulation, accompanied by dysregulated release of soluble mediators. Later stages of IPAH are dominated by vascular remodelling and characterized by enhanced proliferation and extracellular matrix (ECM) synthesis of pulmonary arterial smooth muscle cells (PASMC), with increased endothelial cell apoptosis [4, 5]. Glycosaminoglycans (GAG), a major constituent of the lung ECM, have recently been shown to play a significant role in inflammatory and non-inflammatory lung diseases, exhibiting spatio-temporally distinct effects on epithelial or mesenchymal cell types [8, 9]. GAG regulate hydration and water homeostasis, maintain cell and tissue structure and function, modulate inflammatory responses, and influence tissue repair and remodelling [8, 13]. This led us to hypothesize that differential secretion of GAG by PASMC is associated with vascular remodelling in IPAH.

In this study, we report that IPAH lung tissues exhibit a significantly increased content of hyaluronic acid (HA), the major GAG produced by PASMC. While the relative amount of HA was significantly increased, the content of the sulfated GAG heparan, dermatan, or chondroitin sulphate was decreased, indicating an increased ratio of non-sulfated to sulfated GAG. The increased HA content of IPAH lung tissues was associated with increased and decreased gene expression of hyaluronan synthase (*Has*) 1 and hyaluronoglucosaminidase (*Hyal*) 1, respectively. While we did not relate the HA amount to severity of IPAH (assessed by e.g. PAP or PVR), we are confident that HA exerts a pathophysiologic role, at least in the late and/or severe stages of IPAH that transplant patients exhibit.

Similar changes were observed in primary human PASMC cultured from the lungs of IPAH patients, which demonstrated a significant decrease in *Hyal1* mRNA levels, compared with PASMC obtained from transplant donor lungs. In addition, stimulation of PASMC with TGF-β1, a growth factor involved in the pathogenesis of IPAH [3, 4], led to increased *Has1* gene expression as early as 2 h after stimulation. Since increased HA staining was observed in actively remodelled pulmonary arteries, it is tempting to speculate that HA secretion by PASMC directly influences endothelial and smooth muscle cell proliferation, and may control vasoreactive responses in IPAH.

This is substantiated by the fact that selective overexpression of *Has2* in smooth muscle cells in transgenic mice resulted in significantly increased HA content in the tunica media, enhanced mechanical stiffness and strength, and accelerated development of atherosclerosis [28]. Similar effects were reported for the HA receptor CD44, using CD44-null mice. CD44 expression promoted susceptibility to atherosclerosis, recruitment of macrophages, and smooth muscle cell activation and proliferation [27]. While no pulmonary vascular changes have been investigated in either study, it is highly likely that similar changes in HA and CD44 content in human pulmonary arteries, as reported herein, also affects vascular stiffness and strength, hence further contributing to the increased resistance observed in IPAH.

How are biological effects of HA induced? First, it is known to bind water at 1000-fold of its own weight, hence contributing to tissue hydration and water homeostasis [12, 22, 23]. In addition, increased HA synthesis and turnover represents an early response during lung inflammation in general, and mesenchymal cell activation in particular [8, 12]. HA regulates cell migration, differentiation, and proliferation via interaction with specific cell-surface receptors (CD44 or RHAMM) [12, 22], but also via interaction with toll-like receptors TLR2 and 4 [14]. The interaction of HA with CD44 regulates leukocyte rolling and activation, as

well as tumor metastasis. Furthermore, CD44-dependent clearance of HA fragments is crucial in resolving lung inflammation in the bleomycin model of lung injury [26], demonstrating an essential role for CD44 in the resolution phase of inflammation.

It is of interest to note that the biological effects of HA vary depending on its average molecular mass [12, 23]. Under physiological conditions, HA is a polymer of high average molecular mass above of 106 kDa. In contrast, HA fragments of lower molecular mass accumulate following tissue injury, which are cleared via binding to the cell surface receptor CD44. HA with lower molecular mass ($0.3– 0.5 \times 10^6$ Da) has been reported to prolong the survival of eosinophils *in vitro* [33]. HA of intermediate molecular mass, also termed HA fragments ($<2 \times 10^5$ Da), induces the expression of cytokines, chemokines, or inducible NO synthase by macrophages [34], affects ECM turnover in murine alveolar macrophages [34], and stimulates TGF-β1 synthesis [33]. It has been shown that fragmented HA with an average molecular mass of 250 kDa induces the expression of inflammatory genes [35], while HA of higher molecular weight exhibited the opposite effect and suppressed chemokine expression [23]. Therefore, it would be of interest to elucidate in future studies whether HA expressed in the vascular system of control donor lung specimen is of different average molecular weight than in IPAH specimen. In this context, dysregulation of Has/Hyal expression and/or activity may lead to the generation of HA of different molecular masses thereby exhibiting distinct biological effects, e.g. facilitating PASMC migration and proliferation, that potentially contribute to the pathogenesis of IPAH.

The above described *in vivo* experiments were supported by our observations in primary cultures of PASMC. We found that TGF-β1, but not BMP-2, significantly stimulated total GAG synthesis and HA secretion, an effect which coincided with an increased *Has1* gene expression. The TGF-β1-dependent increase in GAG synthesis was mediated via the Smad and p38 MAP kinase pathways. Our results are in agreement with previous studies in human

fibroblast-like synoviocytes, which have revealed that TGF-β1 is a potent stimulus for *Has1* expression. Furthermore, blocking p38 MAP kinase inhibited TGF-β1-induced *Has1* expression by 90% [36], which underlines that p38 signaling pathway is important for TGF-β1-regulated expression of *Has* isoforms. Since TGF-β1 is a potent stimulus for PASMC migration, *Has1*-mediated HA synthesis may represent a necessary step for PASMC activation and migration. The aforementioned changes in Has/Hyal expression, along with the change in HA synthesis and content in IPAH, may also potentially result from the tissue hypoxia observed in IPAH. Of note, we have previously reported that hypoxia potentiates GAG synthesis induced by TGF-β or PDGF-BB by primary lung fibroblasts [16, 37], suggesting that hypoxia is a synergistic regulator of increased GAG deposition observed in IPAH.

In conclusion, our results demonstrate an increased HA content in IPAH lungs, which was associated with increased *Has1* and decreased *Hyal1* gene expression. Synergistic regulation of GAG metabolizing enzymes in favour of accumulation may thus regulate pathologic remodelling in IPAH by favouring the activation state of PASMC.

FIGURE LEGENDS

FIGURE 1. GAG expression in IPAH and control lung tissue samples. a) Representative cellulose acetate membranes demonstrating the electrophoretic separation of total GAG in donor and IPAH lung specimen. G1 to G4 (left panel) indicate the four detectable GAG peaks in lung tissues, while arrows on the right panel indicate the mobility of commercially available GAG standards: HA, hyaluronic acid; HS, heparan sulphate; DS, dermatan sulphate; CS, chondroitin sulphate. b) Densitometric quantitation of mean ± SEM values of alcian blue staining of the electrophoretic separation of GAG. * indicates $p<0.01$. c) Measurement of the relative content of HA in aliquots of total GAG containing 0.15 µg of uronic acids by EIA. Data are presented as means ± SEM, * indicates $p<0.01$. For all investigations, samples from 4 donor and 5 IPAH lung tissue specimens were used.

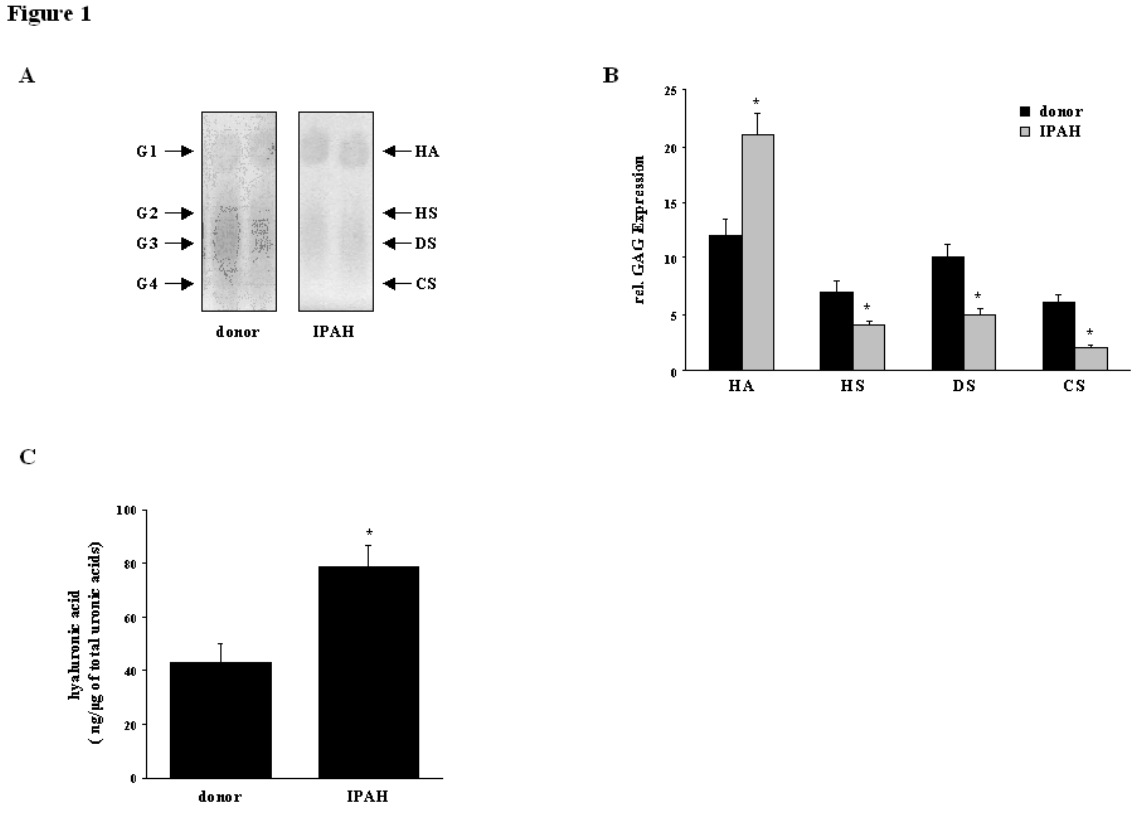

FIGURE 2. Localisation of α-smooth muscle actin (α-SMA), hyaluronic acid (HABP), hyaluronic acid synthase (HAS) 1, and hyaluronoglucosaminidase (HYAL) 1 in pulmonary arteries of control transplant donors and IPAH patients were assessed by immunohistochemistry. HA was visualized by staining with HA-binding protein (HABP), while α-SMA, HAS1, and HYAL1 were stained using specific antibodies. Sections are representative for at least 4 different donors or IPAH patients (magnification × 10). Arrows indicate HYAL1 expression in bronchial and alveolar epithelial type II cells in IPAH (upper panels), arrowheads indicate HA expression in PASMC in remodeled lesions that are negative for α-smooth muscle actin (lower panels).

Figure 2

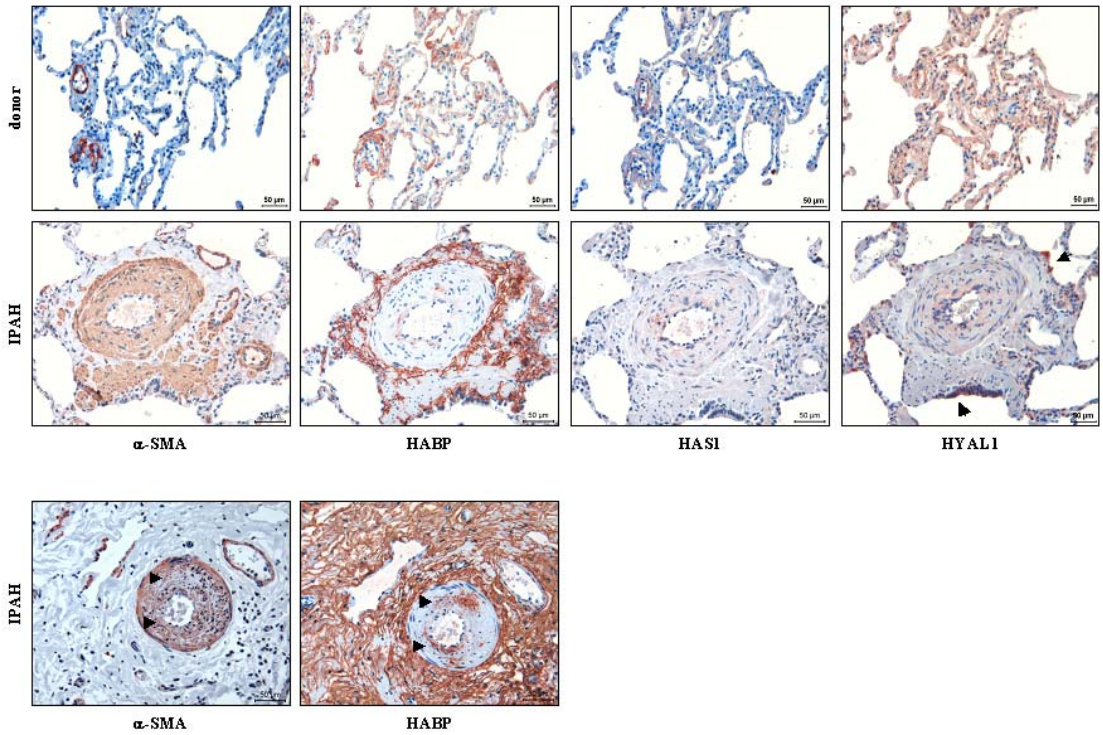

FIGURE 3. Differential expression of *Has1*, *Hyal1*, and *CD44* in lungs of IPAH patients. a) The mRNA was extracted from human lung specimens obtained from IPAH patients (■, n = 12) and donors (□, n=8) and the relative expression levels of *Has1-3*, *Hyal1-4*, *CD44*, and

Rhamm were measured by qRT-PCR. Data are presented as means ± SEM of the relative expression level of the indicated gene and presented as ΔCt values, * indicates p<0.05). b) HAS1 protein levels were investigated in human lung homogenate samples from donors or IPAH patients by Western blotting. GAPDH served as a loading control. Data are representative for at least three independent experiments.

Figure 3

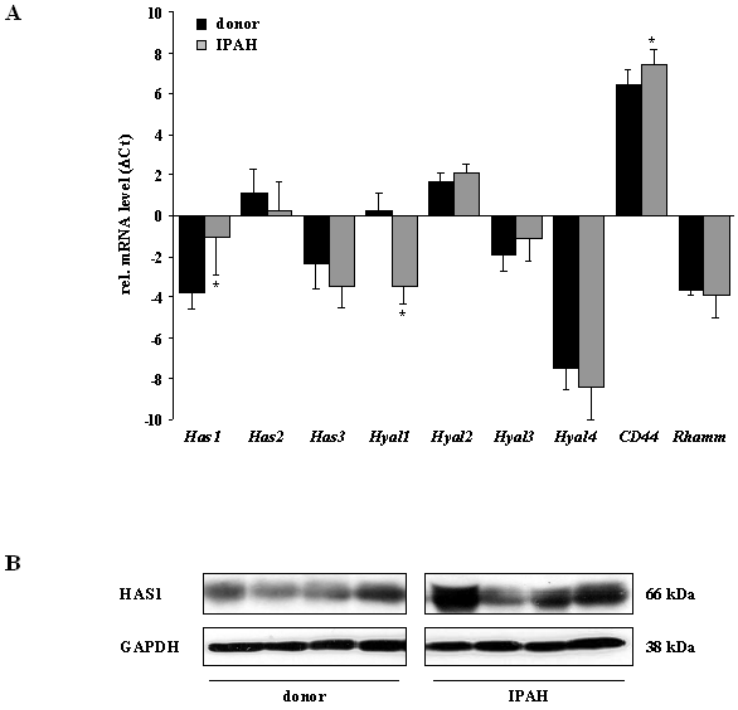

FIGURE 4. Differential expression of *Hyal1* in PASMC derived from the lungs of IPAH patients. The *Has1* and *Hyal1* mRNA levels were assessed in primary PASMC isolated from donors (n=3) and IPAH (n=6) lungs by quantitative real-time PCR (qRT-PCR). Data are presented as means ± SEM of the relative expression level of the indicated gene and presented as ΔCt values., * indicates $p < 0.05$.

Figure 4

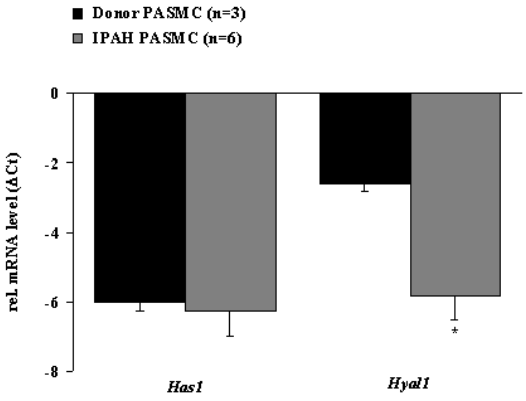

FIGURE 5. Effect of TGF-β1 on GAG secretion and deposition by PASMC. a) subconfluent primary human PASMC were incubated with PDGF-BB, TGF-β1, or BMP-2 for 24 h, in the presence of [^{3}H]-glucosamine at 0.5 μCi/ml. Incorporation of [^{3}H]-glucosamine was then assessed in supernatants (representing secreted GAG) and cell layers (representing deposited GAG), as indicated. b) Subconfluent primary PASMC were stimulated with TGF-β1 in the presence or absence of the p38 kinase inhibitor SB203580 or the type I TGF-β1 receptor kinase inhibitor SB431542, and the incorporation of [^{3}H]-glucosamine was assessed. Data are presented as means ± SEM of [^{3}H]-glucosamine incorporation (n=4 for each). * indicates $p<0.005$ compared with control values; ** indicates $p<0.01$ compared with TGF-β1-stimulated values.

Figure 5

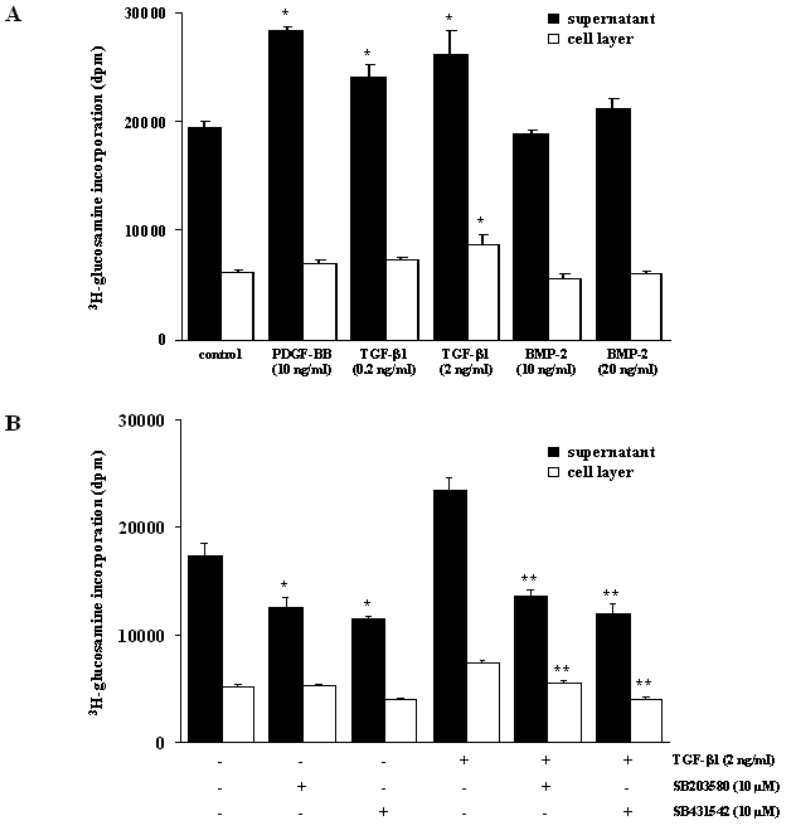

FIGURE 6. Effect of TGF-β1 on HA secretion by PASMC. Subconfluent primary PASMC were incubated with the indicated concentrations of TGF-β1 for 6 to 24 h. HA was measured in cell culture supernatants by EIA. Data are presented as means ± SEM of 4 independent experiments. * indicates $p < 0.001$, ** indicates $p < 0.01$.

Figure 6

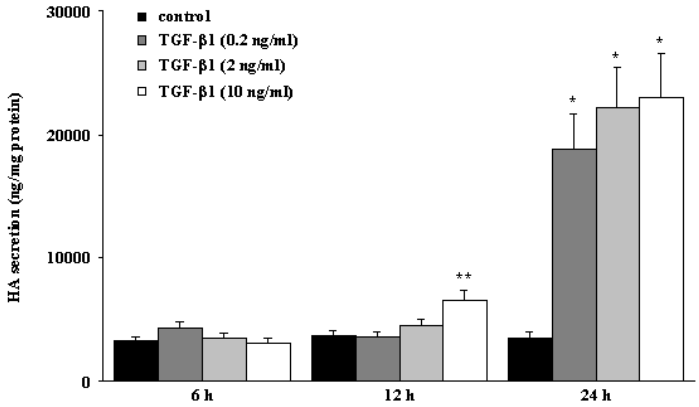

FIGURE 7. Induction of *Has1* gene expression in TGF-β1-stimulated PASMC. The mRNA was extracted from primary human PASMC (n = 3), each stimulated for 2 or 6 h with TGF-β1 (2 ng/ml), and the relative expression levels of *Has1-3*, *Hyal1-3*, *CD44*, and *Rhamm* were determined by qRT-PCR. Data are presented as means ± SEM of the relative expression level of the indicated gene and presented as ΔCt values, * indicates $p<0.001$).

Figure 7

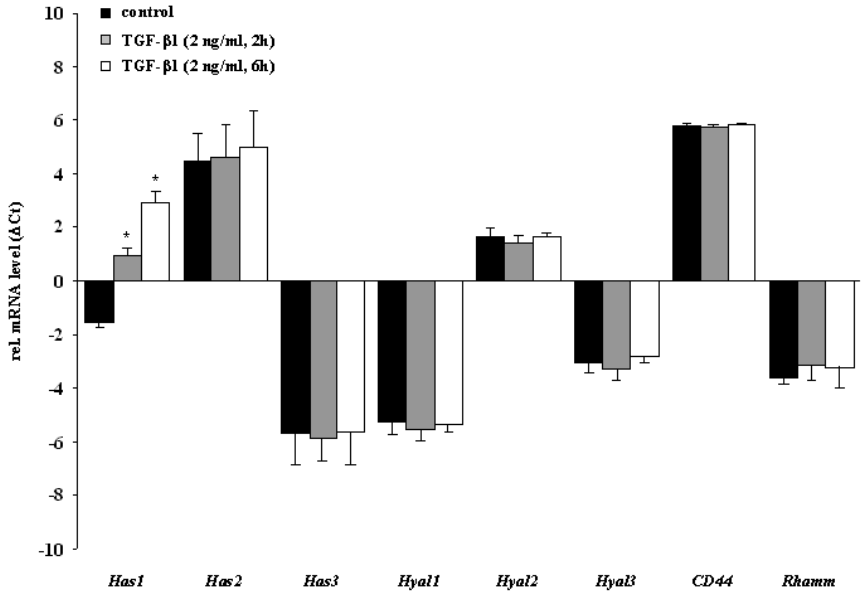
control
TGF-β1 (2 ng/ml, 2h)
TGF-β1 (2 ng/ml, 6h)
rel. mRNA level (ΔCt)
10
8
6
4
2
0
-2
-4
-6
-8
-10
*
*
Has1
Has2
Has3
Hyal1
Hyal2
Hyal3
CD44
Rhamm

Table 1

Characteristics of IPAH patients. PAP = pulmonary arterial pressure, *BMPR2* status = presence (+) or absence (-) of exonic *BMPR2* mutations. n/a = not available

no.	**diagnosis**	**gender**	**age (yr)**	**PAP (mmHg)**	**Treatment**	***BMPR2* status**
1	IPAH	female	26	n/a	n/a	-
2	IPAH	male	21	n/a	Prostacyclin	-
3	IPAH	female	28	95	NO, Bosentan	-
4	IPAH	male	44	83	Prostacyclin	-
5	IPAH	female	52	92	Prostacyclin	-
6	IPAH	male	28	80	Prostacyclin	-
7	IPAH	female	43	n/a	Bosentan	-
8	IPAH	female	40	56	Bosentan	-
9	IPAH	male	45	81	Sildenafil	-
10	IPAH	male	30	95	Remodulin	-
11	IPAH	female	20	n/a	sildenafil	-
12	IPAH	female	12	n/a	na	-

Table 2

Primer sequences and amplicon sizes used for the analysis of human lung tissues and PASMC. All primer sets were designed to work under identical real-time PCR cycling conditions and simultaneous amplifications were obtained in the same run. Sequences were according to GeneBank reference sequences, all accession numbers are given below.

Gene	Accession No.		sequence (5´ → 3´)	length	amplicon size
has 1	NM001523	for	gcgatactgggtagccttca	20 bp	131 bp
		rev	ggttgtaccaggcctcaaga	20 bp	
has 2	NM005328.1	for	acagacaggctgaggacgac	20 bp	126 bp
		rev	ctgtgattccaaggaggag	20 bp	
has 3	NM005329.2	for	gtcatgtacacggccttcaa	20 bp	125 bp
		rev	cctacttggggatcctcctc	20 bp	
hyal 1	NM007312	for	gtgctgccctatgtccagat	20 bp	132 bp
		rev	attttcccagctcacccaga	20 bp	
hyal 2	NM033158	for	tctaccattggcgagagtg	19 bp	119 bp
		rev	gcagccgtgtcaggtaat	19 bp	
hyal 3	NM003549	for	gatctgggaggttcctgtcc	20 bp	110 bp
		rev	agagctggagaggctcaggt	20 bp	
hyal 4	NM012269	for	tgaggatctccaccatgaca	20 bp	134 bp
		rev	ggcagcactttctcctatgg	20 bp	
Cd44	NM000610.3	for	cccagatggagaaagctctg	20 bp	113 bp
		rev	gttgtttgctgcacagatgg	20 bp	
rhamm	NM012484.1	for	gttgtgcaccatctccaggt	20 bp	152 bp
		rev	agctgaagcaggcaaggtag	20 bp	
hmbs	NM000190.3	for	gcacccacacacagcctac	19 bp	108 bp
		rev	gtacccacgcgaatcactct	20 bp	

Table 3

Enzymatic treatment of total GAGs isolated and purified from human lung tissue specimens with GAG-degrading enzymes

Substrate	Chondroitinase ABC	Chondroitinase B	Hyaluronidase	Heparinase	Heparitinase	Keratanase
G1	(-)	(-)	(+)	(-)	(-)	(-)
G2	(-)	(-)	(-)	(-)	(+)	(-)
G3	(+)	(+)	(-)	(-)	(-)	(-)
G4	(+)	(-)	(-)	(-)	(-)	(-)
CSA	(+)	(-)	(-)	(-)	(-)	(-)
DS	(+)	(+)	(-)	(-)	(-)	(-)
CSC	(+)	(-)	(-)	(-)	(-)	(-)
H	(-)	(-)	(-)	(+)	(-)	(-)
HA	(+)	(-)	(+)	(-)	(-)	(-)
HS	(-)	(-)	(-)	(-)	(+)	(-)
KS	(-)	(-)	(-)	(-)	(-)	(+)

Total GAG isolated and purified from human lung tissue specimens of donors (n=5) or IPAH patients (n=5) were treated with the indicated GAG-degrading enzymes. The digestion was monitored by cellulose acetate electrophoresis. Data shown represent observations from five different lung tissue specimens. CSA, chondroitin sulphate A; DS, dermatan sulphate B; CSC, chondroitin sulphate C; H, heparin; HA, hyaluronic acid; HS, heparan sulphate; KS, keratan sulphate. (+): 100% degradation, (-): no detectable degradation. GAG populations G1, G2, G3 and G4 are as obtained following cellulose acetate electrophoresis and numbers correspond to those of figure 1a.

REFERENCES

1. Gaine SP, Rubin LJ. Primary pulmonary hypertension. *Lancet* 1998: 352(9129): 719-725.
2. Humbert M, Sitbon O, Simonneau G. Treatment of pulmonary arterial hypertension. *N Engl J Med* 2004: 351(14): 1425-1436.
3. Eickelberg O, Morty RE. Transforming Growth Factor beta/Bone Morphogenic Protein Signaling in Pulmonary Arterial Hypertension: Remodeling Revisited. *Trends Cardiovasc Med* 2007: 17(8): 263-269.
4. Humbert M, Morrell NW, Archer SL, Stenmark KR, MacLean MR, Lang IM, Christman BW, Weir EK, Eickelberg O, Voelkel NF, Rabinovitch M. Cellular and molecular pathobiology of pulmonary arterial hypertension. *J Am Coll Cardiol* 2004: 43(12 Suppl S): 13S-24S.
5. Olschewski H, Rose F, Grunig E, Ghofrani HA, Walmrath D, Schulz R, Schermuly R, Grimminger F, Seeger W. Cellular pathophysiology and therapy of pulmonary hypertension. *J Lab Clin Med* 2001: 138(6): 367-377.
6. Hassoun PM. Deciphering the "matrix" in pulmonary vascular remodelling. *Eur Respir J* 2005: 25(5): 778-779.
7. Rabinovitch M. Pathobiology of pulmonary hypertension. Extracellular matrix. *Clin Chest Med* 2001: 22(3): 433-449, viii.
8. Noble PW, Jiang D. Matrix regulation of lung injury, inflammation, and repair: the role of innate immunity. *Proc Am Thor Soc* 2006: 3(5): 401-404.
9. Laurent GJ, Chambers RC, Hill MR, McAnulty RJ. Regulation of matrix turnover: fibroblasts, forces, factors and fibrosis. *Biochem Soc Trans* 2007: 35(Pt 4): 647-651.

10. McAnulty RJ, Laurent GJ. Collagen synthesis and degradation in vivo. Evidence for rapid rates of collagen turnover with extensive degradation of newly synthesized collagen in tissues of the adult rat. *Coll Rel Res* 1987: 7(2): 93-104.
11. Bosman FT, Stamenkovic I. Functional structure and composition of the extracellular matrix. *J Pathol* 2003: 200(4): 423-428.
12. Jiang D, Liang J, Noble PW. Hyaluronan in tissue injury and repair. *Ann Rev Cell Dev Biol* 2007: 23: 435-461.
13. Souza-Fernandes AB, Pelosi P, Rocco PR. Bench-to-bedside review: the role of glycosaminoglycans in respiratory disease. *Crit Care* 2006: 10(6): 237.
14. Jiang D, Liang J, Fan J, Yu S, Chen S, Luo Y, Prestwich GD, Mascarenhas MM, Garg HG, Quinn DA, Homer RJ, Goldstein DR, Bucala R, Lee PJ, Medzhitov R, Noble PW. Regulation of lung injury and repair by Toll-like receptors and hyaluronan. *Nat Med* 2005: 11(11): 1173-1179.
15. Papakonstantinou E, Roth M, Kokkas B, Papadopoulos C, Karakiulakis G. Losartan inhibits the angiotensin II-induced modifications on fibrinolysis and matrix deposition by primary human vascular smooth muscle cells. *J Cardiovasc Pharmacol* 2001: 38(5): 715-728.
16. Papakonstantinou E, Karakiulakis G, Tamm M, Perruchoud AP, Roth M. Hypoxia modifies the effect of PDGF on glycosaminoglycan synthesis by primary human lung cells. *Am J Physiol Lung Cell Mol Physiol* 2000: 279(5): L825-834.
17. Hance AJ, Crystal RG. The connective tissue of lung. *Am Rev Resp Dis* 1975: 112(5): 657-711.
18. Itano N, Sawai T, Yoshida M, Lenas P, Yamada Y, Imagawa M, Shinomura T, Hamaguchi M, Yoshida Y, Ohnuki Y, Miyauchi S, Spicer AP, McDonald JA, Kimata

K. Three isoforms of mammalian hyaluronan synthases have distinct enzymatic properties. *J Biol Chem* 1999: 274(35): 25085-25092.

19. Csoka AB, Frost GI, Wong T, Stern R. Purification and microsequencing of hyaluronidase isozymes from human urine. *FEBS Letters* 1997: 417(3): 307-310.
20. Papakonstantinou E, Roth M, Block LH, Mirtsou-Fidani V, Argiriadis P, Karakiulakis G. The differential distribution of hyaluronic acid in the layers of human atheromatic aortas is associated with vascular smooth muscle cell proliferation and migration. *Atherosclerosis* 1998: 138(1): 79-89.
21. Lee JY, Spicer AP. Hyaluronan: a multifunctional, megaDalton, stealth molecule. *Cur Opin Cell Biol* 2000: 12(5): 581-586.
22. Toole BP. Hyaluronan: from extracellular glue to pericellular cue. *Nat Rev Cell Mol Biol* 2004: 4(7): 528-539.
23. Turino GM, Cantor JO. Hyaluronan in respiratory injury and repair. *Am J Resp Crit Care Med* 2003: 167(9): 1169-1175.
24. Turley EA, Noble PW, Bourguignon LY. Signaling properties of hyaluronan receptors. *J Biol Chem* 2002: 277(7): 4589-4592.
25. Day AJ, Prestwich GD. Hyaluronan-binding proteins: tying up the giant. *J Biol Chem* 2002: 277(7): 4585-4588.
26. Teder P, Vandivier RW, Jiang D, Liang J, Cohn L, Pure E, Henson PM, Noble PW. Resolution of lung inflammation by CD44. *Science* 2002: 296(5565): 155-158.
27. Cuff CA, Kothapalli D, Azonobi I, Chun S, Zhang Y, Belkin R, Yeh C, Secreto A, Assoian RK, Rader DJ, Pure E. The adhesion receptor CD44 promotes atherosclerosis by mediating inflammatory cell recruitment and vascular cell activation. *J Clin Invest* 2001: 108(7): 1031-1040.

28. Chai S, Chai Q, Danielsen CC, Hjorth P, Nyengaard JR, Ledet T, Yamaguchi Y, Rasmussen LM, Wogensen L. Overexpression of hyaluronan in the tunica media promotes the development of atherosclerosis. *Circ Res* 2005: 96(5): 583-591.

29. Goueffic Y, Guilluy C, Guerin P, Patra P, Pacaud P, Loirand G. Hyaluronan induces vascular smooth muscle cell migration through RHAMM-mediated PI3K-dependent Rac activation. *Cardiovasc Res* 2006: 72(2): 339-348.

30. Zakrzewicz A, Hecker M, Marsh LM, Kwapiszewska G, Nejman B, Long L, Seeger W, Schermuly RT, Morrell NW, Morty RE, Eickelberg O. Receptor for activated C-kinase 1, a novel interaction partner of type II bone morphogenetic protein receptor, regulates smooth muscle cell proliferation in pulmonary arterial hypertension. *Circulation* 2007: 115(23): 2957-2968.

31. Bitter T, Muir HM. A modified uronic acid carbazole reaction. *Anal Biochem* 1962: 4: 330-334.

32. Papakonstantinou E, Karakiulakis G, Roth M, Block LH. Platelet-derived growth factor stimulates the secretion of hyaluronic acid by proliferating human vascular smooth muscle cells. *Proc Natl Acad Sci USA* 1995: 92(21): 9881-9885.

33. Ohkawara Y, Tamura G, Iwasaki T, Tanaka A, Kikuchi T, Shirato K. Activation and transforming growth factor-beta production in eosinophils by hyaluronan. *Am J Resp Cell Mol Biol* 2000: 23(4): 444-451.

34. McKee CM, Penno MB, Cowman M, Burdick MD, Strieter RM, Bao C, Noble PW. Hyaluronan (HA) fragments induce chemokine gene expression in alveolar macrophages. The role of HA size and CD44. *J Clin Invest* 1996: 98(10): 2403-2413.

35. Tammi MI, Day AJ, Turley EA. Hyaluronan and homeostasis: a balancing act. *J Biol Chem* 2002: 277(7): 4581-4584.

36. Stuhlmeier KM, Pollaschek C. Differential effect of transforming growth factor beta (TGF-beta) on the genes encoding hyaluronan synthases and utilization of the p38 MAPK pathway in TGF-beta-induced hyaluronan synthase 1 activation. *J Biol Chem* 2004: 279(10): 8753-8760.

37. Papakonstantinou E, Roth M, Tamm M, Eickelberg O, Perruchoud AP, Karakiulakis G. Hypoxia differentially enhances the effects of transforming growth factor-beta isoforms on the synthesis and secretion of glycosaminoglycans by human lung fibroblasts. *J Pharmacol Exp Ther* 2002: 301(3): 830-837.